Received: 12 August 2022 | Revised: 17 April 2023 | Accepted: 12 June 2023

DOI: 10.1002/jez.b.23214

RESEARCH ARTICLE

JEZ-B MOLECULAR AND DEVELOPMENTAL EVOLUTION WILEY

Embryonic pattern of cartilaginous head development in the European toad, *Bufo bufo*

Paul Lukas

Institute of Zoology and Evolutionary Research, Friedrich-Schiller-University Jena, Jena, Germany

Correspondence
Paul Lukas, Institute of Zoology and Evolutionary Research, Friedrich-Schiller-University Jena, Jena, Germany.
Email: paul.lukas@uni-jena.de

Funding information
Deutsche Forschungsgemeinschaft

Abstract

The craniofacial skeleton of vertebrates is a major innovation of the whole clade. Its development and composition requires a precisely orchestrated sequence of chondrification events which lead to a fully functional skeleton. Sequential information on the precise timing and sequence of embryonic cartilaginous head development are available for a growing number of vertebrates. This enables a more and more comprehensive comparison of the evolutionary trends within and among different vertebrate clades. This comparison of sequential patterns of cartilage formation enables insights into the evolution of development of the cartilaginous head skeleton. The cartilaginous sequence of head formation of three basal anurans (*Xenopus laevis*, *Bombina orientalis*, *Discoglossus scovazzi*) was investigated so far. This study investigates the sequence and timing of larval cartilaginous development of the head skeleton from the appearance of mesenchymal Anlagen until the premetamorphic larvae in the neobatrachian species *Bufo bufo*. Clearing and staining, histology, and 3D reconstruction enabled the tracking of 75 cartilaginous structures and the illustration of the sequential changes of the skull as well as the identification of evolutionary trends of sequential cartilage formation in the anuran head. The anuran viscerocranium does not chondrify in the ancestral anterior to posterior direction and the neurocranial elements do not chondrify in posterior to anterior direction. Instead, the viscerocranial and neurocranial development is mosaic-like and differs greatly from the gnathostome sequence. Strict ancestral anterior to posterior developmental sequences can be observed within the branchial basket. Thus, this data is the basis for further comparative developmental studies of anuran skeletal development.

KEYWORDS

Bufonidae, chondrocranium, developmental patterning, developmental sequence, neurocranium, viscerocranium

1 | INTRODUCTION

The lissamphibians are the most basal representatives of the tetrapods. They consist of the three extant orders including Gymnophiona, Caudata, and Anura. Among them, anurans dominate in terms of species numbers (Pyron, 2014). The biphasic lifestyle, which is typical for the majority of anuran species, facilitates the presence of two life phases connected by a metamorphosis (McDiarmid & Altig, 1999). During this relatively short period the morphology as well as behavior, diet and habitat preferences change drastically (Wassersug, 1975; Handrigan & Wassersug, 2007; Harrington et al., 2013). This enables the independent exploitation of different resources during the larval and adult periods, and it leads to two distinct developmental sections which are a rich source for developmental investigations. Especially the craniofacial skeleton undergoes numerous changes during ontogenesis. It consists of three components, the dermatocranium, the neurocranium, and the viscerocranium. The dermatocranium includes most of the plate-like bones and is of mixed embryological origin (neural crest and mesodermal) (Franz-Odendaal et al., 2006). The viscerocranium, which is derived from the neural crest, comprises the skeleteal elements of the mandibular, hyoid, and gill arches (Cerny et al., 2006; Kuratani et al., 1997). The neurocranium is also of mixed origin and encapsulates the brain and the sensory organs (Couly et al., 1992). Neural crest cells are responsible for the formation of major part of the larval head skeleton, which initially only consists of viscerocranial and neurocranial derivatives in amphibians (Gross & Hanken, 2008; Olsson & Hanken, 1996). The shape and fate of these cells largely depends on partitioning of the precursor cell populations along the anteroposterior and dorsoventral axes mediated by different genetic factors (Depew et al., 2002; Kuratani, 2012). The development of the anuran craniofacial skeleton is initiated by the aggregation of mesenchymal cells which start to interact with an epithelium. This marks the site of future skeletogenesis (Hall & Miyake, 1995, 2000). Later the condensed cells begin to differentiate into chondroblasts and during further development into chondrocytes. They undergo maturation which results in cartilage formation (Goldring et al., 2006). Predominantly, the cartilaginous chondrocranium is the earliest functional skeletal element to form (Rose, 2009). It enables food acquisition and additional capabilities. Therefore, the proper development of the chondrocranium is fundamental to successful further development. Despite their relatively uniform body plan, anuran tadpoles exhibit an overwhelming skeletal diversity, regarding the form, position, and existence of specific cartilages as well as the specific order in which they develop. The differences in the larval skeleton among different anuran species must be caused by different developmental processes. The investigation of developmental sequences should shed light on the different patterns during the chondrocranial development which led to different skeletal morphologies.

The sequence of chondrocranial development and the identification of similarities and differences among different taxa is a rich source for the understanding of the evolution of development. Evolutionary changes as for example heterochronic shifts and ontogenetic novelties, can be revealed and the developmental features can be taxonomically important and helpful in cladistic analyses. A growing number of descriptions of the chondrocranial development became available in recent decades. The development of numerous species from all major vertebrate clades was described and specific traits identified (Dutel et al., 2019; Gillis et al., 2009, 2012; Hernández-Jaimes et al., 2012; Kuratani, 1999; Langille & Hall, 1987; Lukas & Olsson, 2018; Ollonen et al., 2018; Tulenko & Sheil, 2007; Warth et al., 2017; Werneburg & Yaryhin, 2019). The skull of birds and squamates chondrifies in anterior to posterior direction (Dutel et al., 2019; Hernández-Jaimes et al., 2012; Werneburg & Yaryhin, 2019). The same goes for the viscerocranium of teleosts and chondrichthyes (Gillis et al., 2009, 2012; Langille & Hall, 1987; Warth et al., 2017). Investigations on the chondrocranial development of larval anurans are scarce, but their number is growing. The developmental sequence of three basal frog species, two discoglossoids (*Bombina orientalis*, *Discoglossus scovazzi*) and one pipoid (*Xenopus laevis*), was recently described and developmental patterns identified (Lukas & Olsson, 2018, 2020; Lukas & Ziermann, 2022). The development of the viscerocranial elements does not follow the anterior to posterior direction as described in other vertebrate clades. Especially derivatives of the mandibular and hyoid arches differ from this sequence. The hyoid arch derived ceratohyal corpus develops before, or simultaneous to mandibular arch derivatives like Meckel's cartilage or infrarostral cartilage. An almost strict anterior to posterior developmental sequence can be observed in the development of the branchial apparatus. Additionally, the development of the neurocranial elements also does not follow the presumably ancestral anterior to posterior direction. Instead, the posterior elements extend anteriorly and the anterior elements extend posteriorly until both parts meet and fuse (Lukas & Olsson, 2018, 2020; Lukas & Ziermann, 2022). In all investigated anurans so far, the neurocranium-anchoring processes of the palatoquadrate chondrify in anterior to posterior direction; first the quadratocranial commissure, then the ascending process, and last the larval otic process. These features of anuran chondrogenesis are a good starting point but they suffer from a relatively small number of investigated taxa. Sequential data of chondrocranial development in the Neobatrachian clade is still missing and will be helpful to further confirm or even refute these features.

Bufonidae is the fifth largest family of anurans. There are 638 species in 52 genera; 21 species are present in the genus *Bufo*. Species of Bufonidae are distributed all over the world and display a variety of developmental modes including the typical aquatic larva, direct development, and viviparity (Angel & Lamotte, 1944). The majority of bufonid tadpoles are generalized pond feeders (Seale & Wassersug, 1979), which feed mostly on algae (Diaz-Paniagua, 1989). First developmental descriptions of *Bufo bufo* were published by Parker in the 19th century (Parker, 1876). The tadpole of *B. bufo* is macrophagous and feeds by taking larger bites of macrophytes and algae attached to submerged substrates (Bonacci et al., 2008;

Savage, 1950). The information gained from the developmental sequence of *B. bufo* is important as it solidifies common features and changes during chondrocranial development. These changes are of interest as they contain information about evolutionary processes leading to the observed diversities in chondrocranial development. Chondrocranial development has not been studied in any species in Bufonidae and, so far, only one larval skeletal feature, the presence of a dorsal connection from the muscular process to the quadratocranial commissure is described as a synapomorphy of bufonids (excluding *Melanophryniscus*) (Frost et al., 2006). Thus, the investigation of their skeletal development and the comparison to available data on anuran chondrocranial development will add another piece of knowledge to further uncover the ancestral mode of anuran skeletal development.

The present work provides a comprehensive and illustrated overview of the chondrocranial development of *B. bufo* from the initial mesenchymal Anlagen until the premetamorphic cartilaginous head skeleton. The results are compared to other available developmental studies in anurans to gain further insights into the respective developmental mode. This overview follows and completes recent studies of anuran chondrocranial development and encourages scientists perform more developmental studies of larval cranial morphology, instead of relying on the description of single stages.

2 | METHODS

2.1 | Specimen acquisition and staging

All specimens used in this study are part of the departmental collection. The embryos and larvae were stored in 70% ethanol. They were staged according to the simplified staging table for anuran embryos and larvae (Gosner, 1960) and denominated as "Go stages." A developmental series was established by choosing embryos and larvae from defined stages between Go 20 and Go 35 ($n = 141$). Histological sections ($n = 51$) and cleared-and-stained larvae ($n = 90$) are kept at the Institute of Zoology and Evolutionary Research, Friedrich-Schiller-University, Jena, Germany.

2.2 | Tissue staining

The specimens were dehydrated, embedded in paraffin, and serially sectioned at 7 µm thickness using a rotary microtome (Microm, HM 355 S). The sections were stained according to Heidenhain's Azan technique (Heidenhain, 1915). Images were taken with a Hitachi HV-F202SCL camera mounted on a Zeiss AxioScan Z1 microscope operated with Zen 3.1 software. The clearing-and-staining procedure followed the protocol by Dingerkus and Uhler (1977) with the exception that no alizarin red was used due to the absence of bones in the stages investigated. Cleared-and-stained specimens were examined with a Zeiss Stemi 11 and images were taken with an attached camera (ColorView) operated by AnalySIS software.

2.3 | Image processing

The digitized images (TIFF-format) of the respective histological sections were taken and later exported to Fiji Software (Schindelin et al., 2012). The section images of each individual were stacked and aligned using first the least squares (rigid) and second the elastic nonlinear block correspondence mode from the TrakEM2 plugin for Fiji (Cardona et al., 2012). The resulting aligned stacks were exported in the tagged image file format (TIFF). Skeletal structures were segmented using the Amira 6.0.1. 3D analysis software (FEI Visualization Sciences Group). Polygonal surfaces were rendered and then exported to Wavefront OBJ file format for further processing in Autodesk Maya 2022 (Autodesk, Inc.). Surfaces were smoothed, polygonal counts reduced, and the surfaces arranged. For the final composition, coloring and rendering of images, Autodesk Mudbox 2022 (Autodesk, Inc.) was used. All images were edited and arranged using Adobe Photoshop CS6 and Adobe Illustrator CS6 (Adobe Inc.).

2.4 | Scoring

I evaluated a total of 75 cartilaginous structures, which were defined in my previous work (Lukas & Ziermann, 2022), of 141 specimens. A total of 45 out of 75 characters were identified in *B. bufo*. Terminology used here follows the guidelines introduced by Haas (2003) for cartilaginous features (anglicized terms). The following four different states of cartilaginous development were scored: (1) cartilaginous structures are absent; (2) mesenchymal Anlagen are visible as condensed cell clusters; (3) chondroblasts form condensed precartilaginous cell clusters with clearly visible nuclei; and (4) chondrocytes rich in cytoplasm and bordered by a clearly visible perichondrium are present. All structures were scored after the first appearance principle. If a certain state was visible within the respective structure, the whole structure was scored in this state even if parts of the structure remained in an earlier state. Additionally, I used the previously defined three different stages of development (Lukas & Ziermann, 2022). Each stage is defined by a specific combination of cartilages in different cartilaginous developmental states. A1 (Anlage 1) starts with the appearance of the first mesenchymal Anlage, D1 (Differentiation 1) starts with the appearance of the first Anlage which contains chondroblasts and stage C1 (Cartilage 1) starts with the appearance of the first chondrocyte containing cartilage. The following enumeration of stages is the result of additional cartilaginous structures entering different states.

3 | RESULTS

Based on histological sections and the cleared and stained specimens, I scored the cartilaginous structures and defined 18 substages between Go21 and Go35. The respective state of each cartilaginous structure at each developmental stage are presented in summarized form in Table 1. The external morphology of tadpoles of the same

TABLE 1 Sequence of chondrocranial development in *Bufo bufo*.

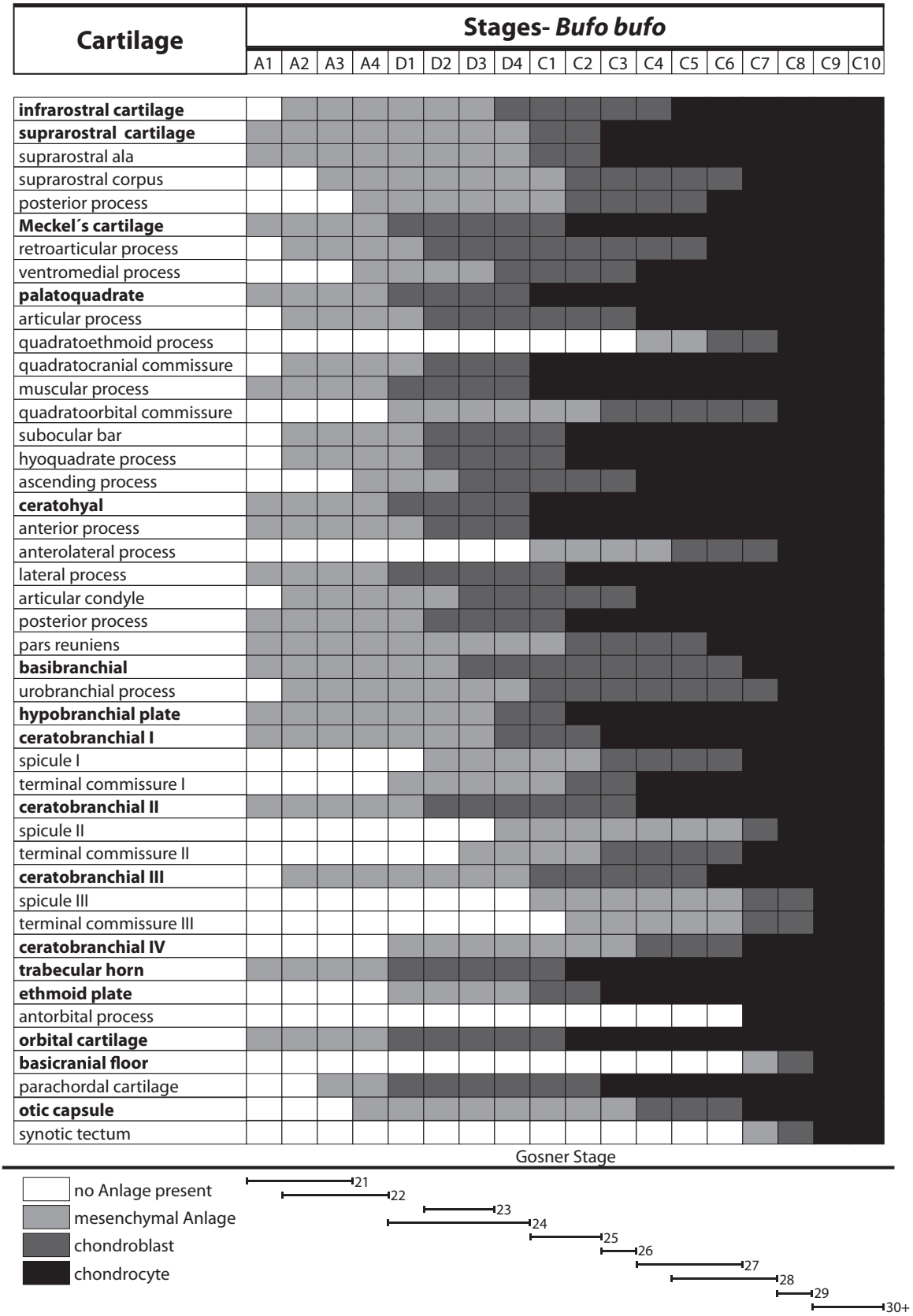

Gosner stage sometimes differs greatly in the progress of skeletogenesis. Especially Gosner stages 21 and 22, as well as Gosner stages 23 and 24 overlap largely in terms of cartilaginous development (Table 1). As reported before in other anuran species (Lukas & Olsson, 2018), conclusions about the skeletal state cannot be drawn from the external development of *B. bufo*.

3.1 | Infrarostral cartilage

The anuran lower jaw consists of two cartilages. The anteriormost is the infrarostral cartilage (Figure 1a). In premetamorphic tadpoles of *B. bufo* the infrarostral cartilage is a single, u-shaped cartilage. Medially, a synchondrosis is present between the lateral parts of this cartilage (Figure 1a). Its lateral parts articulates with Meckel's cartilage via the intramandibular joint. Additionally, the intramandibular commissure connects the dorsolateral part of the infrarostral cartilage with the mediodorsal part of Meckel's cartilage. The bipartite mesenchymal Anlage of the infrarostral cartilage develops at stage A2. It arises between the medial tips of the Anlagen of Meckel's cartilage dorsal to the Musculus (M.) intermandibularis and ventral to the midline of the pharyngeal cavity. During the further stages the Anlagen extend dorsolaterally and fuse medially. The Anlage remains mesenchymal until stage D3 (Figure 1a). At stage D4 chondroblasts begin to differentiate and condense within the Anlage and form a u-shaped band between the medial tips of Meckel's cartilage (Figure 2, see also Figure 3a for the orientation of the cross section). The cartilage further elongates dorsolaterally and the median synchondrosis becomes visible at stage C2. The infrarostral cartilage chondrifies later than several derivatives of the hyoid and branchial arches at stage C5 when the intramandibular joint is also properly developed at the dorsolateral tip. At stage C8 the intramandibular commissure develops dorsolaterally and connects the infrarostral cartilage with Meckel's cartilage.

3.2 | Suprarostral cartilage

The suprarostral cartilage of *B. bufo* is a single cartilage and consists of a median U-shaped corpus which is connected to the trabecular horns via the rostrotrabecular joint and two lateral alae (Figure 1a). The alae emerge from the dorsolateral margins of the corpus. They proceed posteriorly and have a plate-like shape. Both alae bear a posterior process on its posterodorsal margin. An anterior process, as often found in other anuran larvae, is not present. The alae of the suprarostral are among the first mesenchymal Anlagen which appear during chondrogenesis. The Anlagen of each ala are visible as small spheres at the anteriormost and dorsolateral margin of the pharyngeal cavity at stage A1. Until stage A3 they develop into dorsoventrally oriented rods which border the lateral margin of the pharyngeal cavity (Figure 2). At the same stage the mesenchymal

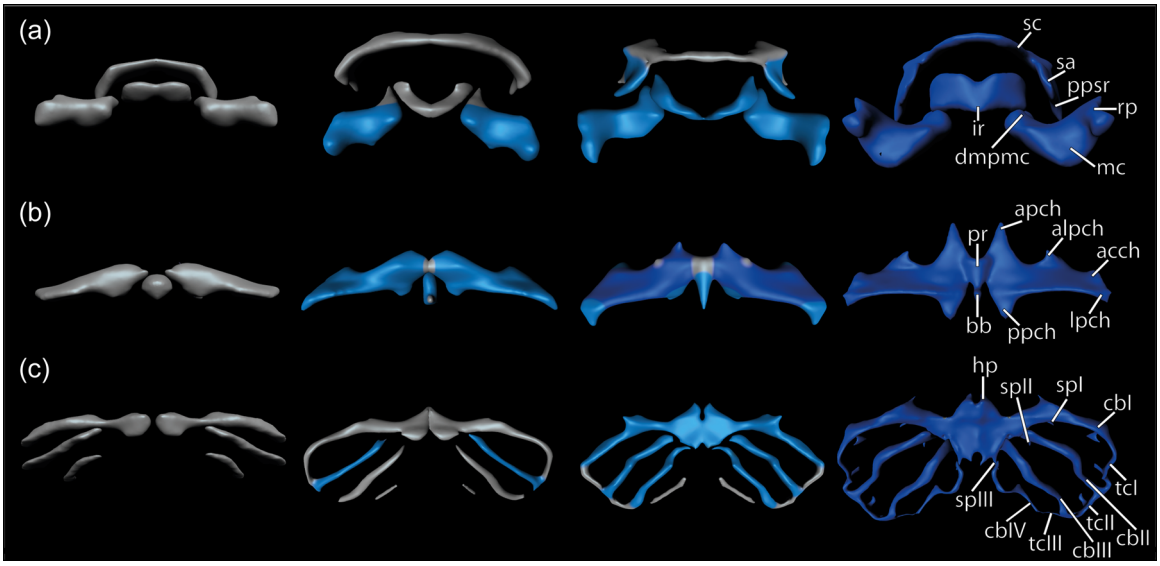

FIGURE 1 3D reconstructions of the head skeleton of *Bufo bufo* larvae showing the cartilaginous development of the mandibular derivatives (a), ceratohyal and basibranchial (b), and the branchial basket (c) during Stages A3, D3, C1, and C9 (left to right) in ventral view. The 3D reconstructions are color-coded, according to the distinct stage of cartilaginous development: "Light gray" means Anlagen are visible as mesenchymal cell clusters; "light blue" means that condensed precartilaginous cell clusters containing chondroblasts are visible, "dark blue" means that the respective cartilage contains chondrocytes rich in cytoplasm and bordered by a distinct perichondrium. Sizes were adjusted. ac, articular condyle; alpch, anterolateral process of ceratohyal; apch, anterior process of ceratohyal; bb, basibranchial; cbI-IV, ceratobranchial I–IV; dmpmc, dorsomedial process of Meckel's cartilage; hp, hypobranchial plate; ir, infrarostral cartilage; lp, lateral process; ch; mc, Meckel's cartilage; ppch, posterior process of ceratohyal; ppsr, posterior process of suprarostral; rp, retroarticular process; sa, suprarostral ala; sc, suprarostral corpus; spI–III, spicule I–III; tcI–III, terminal commissure I–III.

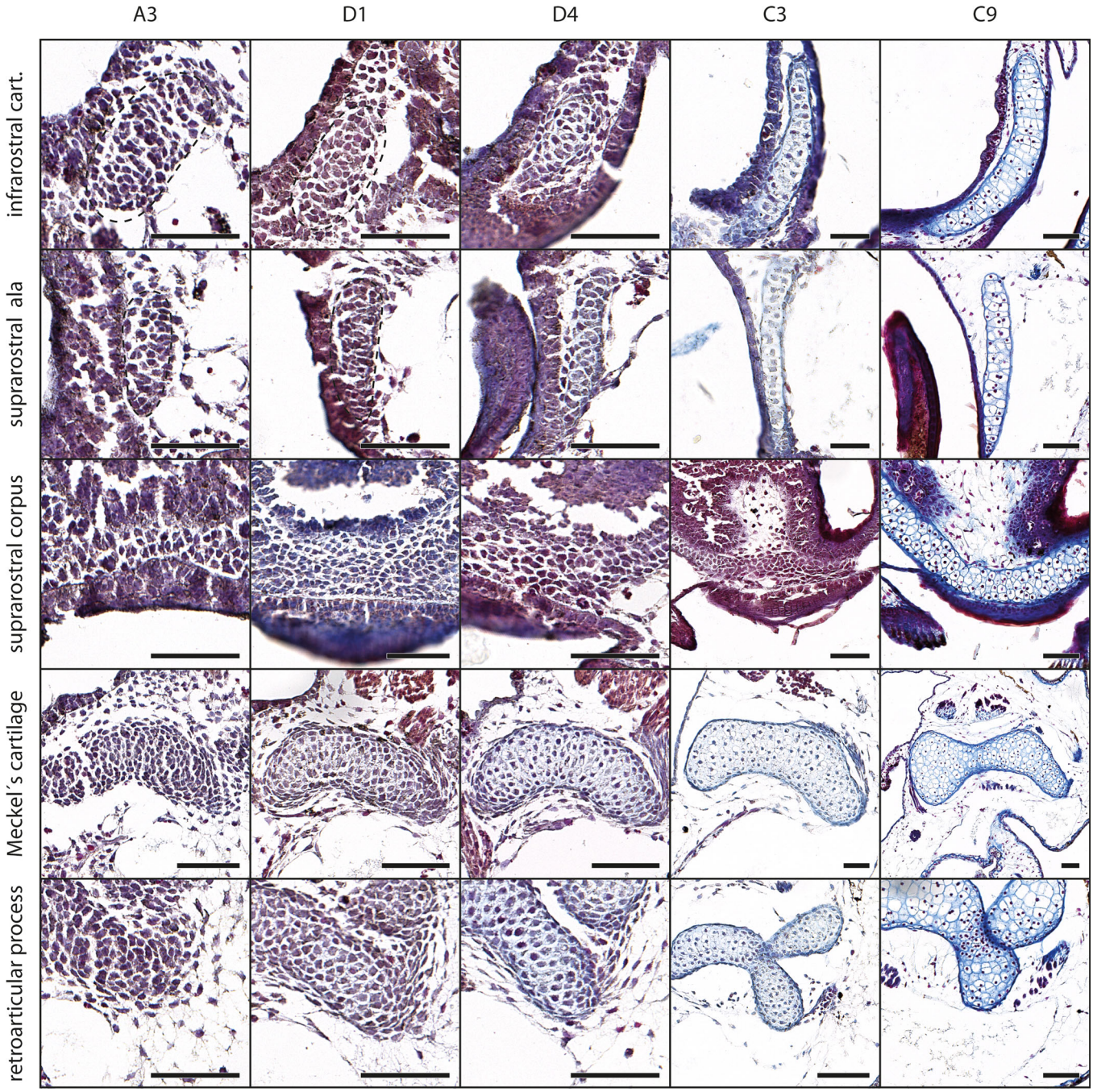

FIGURE 2 *Bufo bufo*, cartilaginous development of mandibular arch derived structures. Azan-stained, transverse histological sections of stage A3 (first column), stage D1 (second column), stage D4 (third column), stage C3 (fourth column), and stage C9 (fifth column) show the chondrification process of the infrarostral cartilage (cart.), the suprarostral ala, the suprarostral corpus, Meckel's cartilage and the retroarticular process of Meckel's cartilage. Difficult observable structures are highlighted by dashed lines. Relative positions of the cross sections are shown in Figure 3a. Scale bars indicate 100 µm.

Anlage of the suprarostral corpus arises beneath the anteroventral margin of the pharyngeal cavity (Figure 2). The Anlage of the corpus connects the Anlagen of the alae. The Anlage of the posterior process emerges from the posterodorsal tip of the ala at stage A4. Whereas other structures differentiate into chondrocytes at stage C1, the suprarostral alae begin to condense and differentiate into chondroblasts during this period (Figure 1a). The suprarostral corpus and the posterior process of the alae follow at stage C2. The alae consist of chondroblast for only two stages and the differentiation into chondrocytes takes place at stage C3 (Figure 2). The suprarostral corpus and the posterior processes of the alae chondrify late at stage C7 and stage C6, respectively.

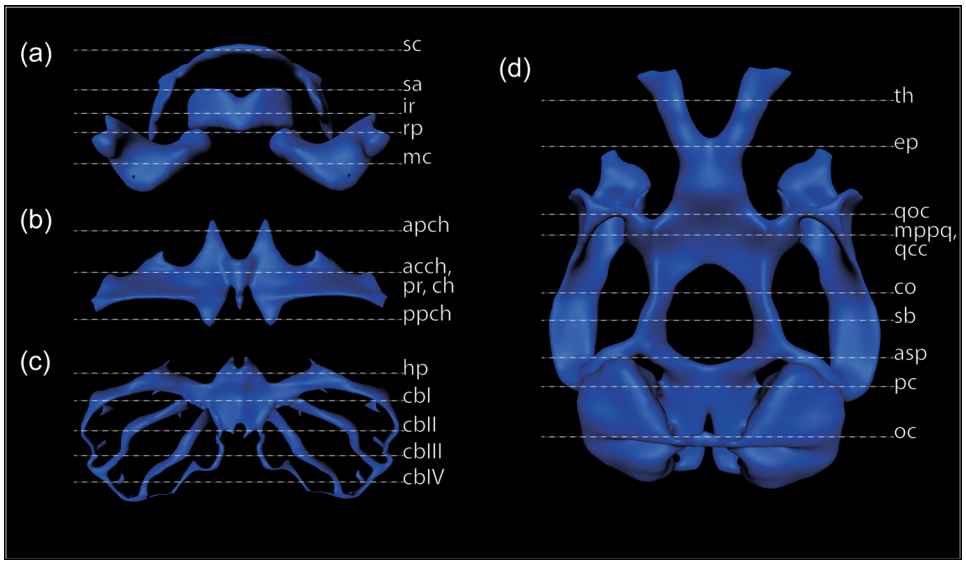

FIGURE 3 Relative position of the cross sections shown in Figure 2 (a), Figure 4 (b), Figure 5 (c), and Figures 6 and 7 (d). acch, articular condyle of ceratohyal; apch, anterior process of ceratohyal; asp, ascending process; cbI–IV, ceratobranchial I–IV; ch, ceratohyal; co, orbital cartilage; ep, ethmoid plate; hp, hypobranchial plate; ir, infrarostral cartilage; mc, Meckel's cartilage; mppq, muscular process of palatoquadrate; oc, otic capsule; pc, parachordal cartilage; ppch, posterior process of ceratohyal; pr, pars reuniens; qcc, quadratocranial commissure; qoc, quadratoorbital commissure; rp, retroarticular process; sa, suprarostral ala; sb, subocular bar; sc, suprarostral corpus; th, trabecular horn.

3.3 | Meckel's cartilage

Meckel's cartilage is the second cartilage of the anuran lower jaw (Figure 1a). It is situated posterolaterally to the infrarostral cartilage and is connected via the mandibular joint to the palatoquadrate. Two processes are present. The ventromedial process establishes the articulation with the infrarostral cartilage and the retroarticular process establishes the articulation with the palatoquadrate. Meckel's cartilage of *B. bufo* has the typical sigmoid shape and is horizontally oriented. The mesenchymal Anlagen of Meckel's cartilage arise early during skeletogenesis at stage A1. Two distinct Anlagen which are shaped like a flattened N are visible at the ventrolateral margin of the pharyngeal cavity. They further extend laterally and medially and enclose the Anlage of the infrarostral cartilage at stage A2. Now the median distance between both Anlagen of Meckel's cartilage enlarges. The mesenchymal Anlagen of the retroarticular process and the ventromedial process develop at stage A2 and A4, respectively (Figure 2). Both are visible as small protruding spheres. The mesenchymal Anlage of Meckel's cartilage is the first to differentiate into chondroblasts at stage D1 (Figure 2). The retroarticular process follows at stage D2 and the ventromedial process at stage D4. Both the intramandibular joint and the mandibular joint begin to develop during these stages and proper articulation is established from stage C1 onwards. Meckel's cartilage chondrifies at stage C2 and acquires its typical shape which does not change until stage C10 (Figure 1a). Despite developing mesenchymal Anlagen and differentiating into chondroblasts after the retroarticular process, the ventromedial process chondrifies at stage C4 whereas the retroarticular process only chondrifies by stage C6.

3.4 | Palatoquadrate

The palatoquadrate is the dorsalmost element of the mandibular arch. Its articular process forms the jaw joint with the retroarticular process of Meckel's cartilage. The palatoquadrate is bordered by the otic capsule posteriorly and by the neurocranial derivatives encapsulating the brain medially (Figure 8). The palatoquadrate of *B. bufo* consists of only two processes which connects it to the neurocranium, the quadratocranial commissure and the ascending process (Figure 8). A larval otic process, as commonly found in other anuran larvae, is absent. The single mesenchymal Anlage of the muscular process of the palatoquadrate arises at stage A1 posterior to the Anlage of Meckel's cartilage and lateral to the pharyngeal cavity. The anterior part of the Anlage is cylindrical, horizontally oriented, and shaped like a depressed U. The posterior part is oblique and is dorsally bordered by the Anlage of the mandibular levator muscles. The Anlage of the muscular process extends posteriorly during further development. At stage A2 the mesenchymal Anlagen of the articular process, quadratocranial commissure, subocular bar, and hyoquadrate process are clearly distinguishable. The quadratocranial commissure extends mediodorsally and fuses with the Anlage of the orbital cartilage at stage A3 (Figures 8a and 6). The muscular process extends further dorsally and surrounds the Anlage of the mandibular levator muscles ventrally and laterally, while the subocular bar grows posteriorly. At stage A4 the ascending process becomes visible as a posterodorsal outgrowth of the subocular bar. Until stage A5 the dorsal tip of the muscular process bends medially. At stage D1 the muscular process is among the first structures which consists of chondroblasts. The dorsal tip of the muscular process is now connected with the orbital cartilage

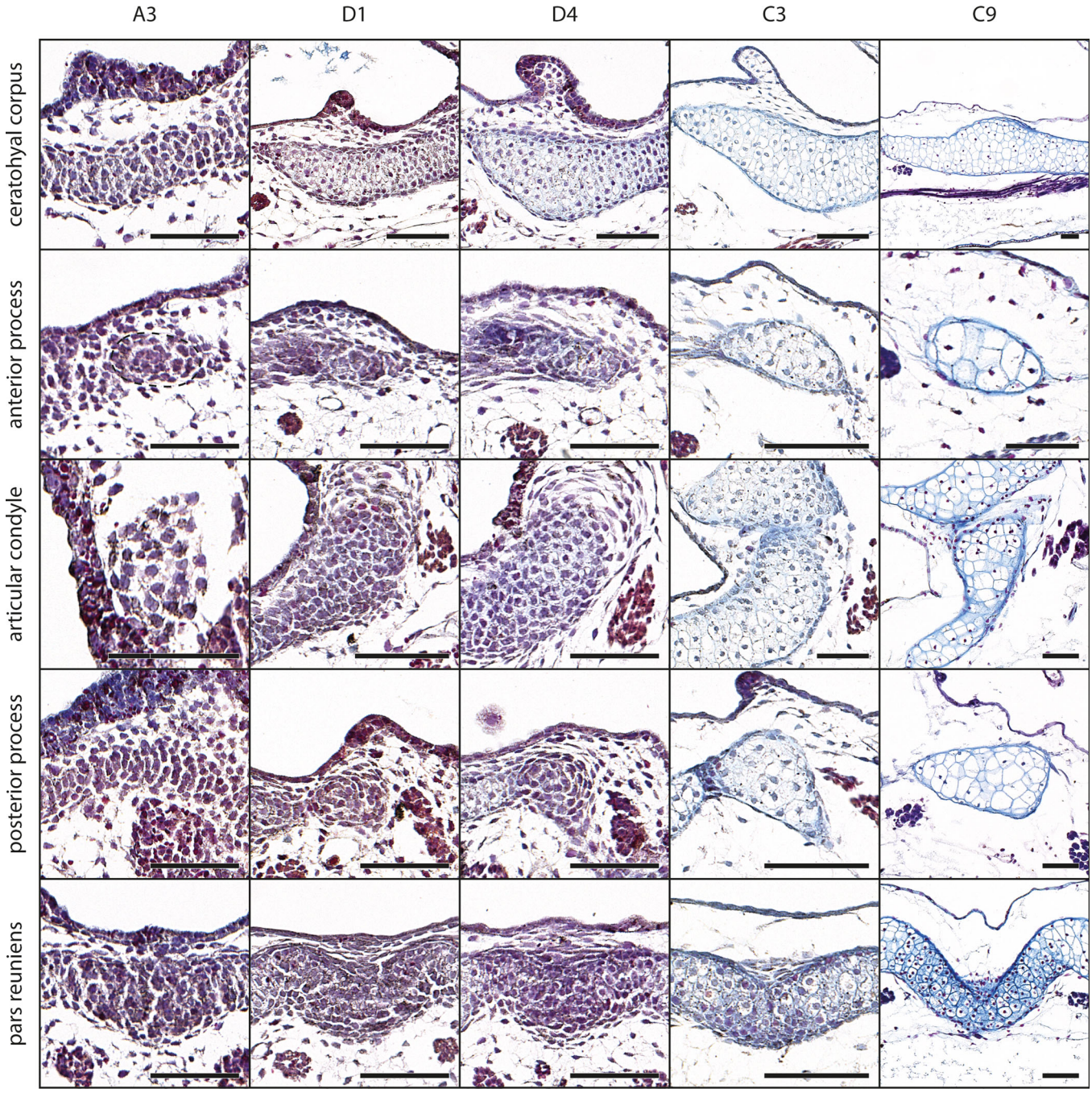

FIGURE 4 *Bufo bufo*, cartilaginous development of the ceratohyal. Azan-stained, transverse histological sections of Stage A3 (first column), stage D1 (second column), stage D4 (third column), stage C3 (fourth column), and stage C9 (fifth column) show the chondrification process of the ceratohyal corpus, the anterior process, the articular condyle, the posterior process and the pars reuniens. Difficult observable structures are highlighted by dashed lines. Relative position of the cross sections is shown in Figure 3b. Scale bars indicate 100 μm.

via the mesenchymal Anlage of the quadratoorbital commissure. Except the ascending process and the quadratoorbital commissure all elements of the palatoquadrate consist of chondroblasts at stage D2. The ascending process follows at stage D3 (Figure 8). The last structure of the palatoqudrate to consist of chondroblasts is the quadratoorbital commissure, which is also the last structure to chondrify. The medial part of the subocular bar is more spherical whereas its lateral tip is a slender bar. During further development the subocular bar changes its orientation from horizontal to oblique, extending from medioventral to dorsolateral. The muscular process and the quadratocranial commissure are among the first elements to chondrify at stage C1 (Figure 8). Together, the two cartilages enclose the mandibular levator muscles. At stage C2 the hyoquadrate process and the subocular bar consist of chondrocytes. Together with the articular condyle of the ceratohyal the hyoquadrate process of the palatoquadrate forms a proper joint, at which

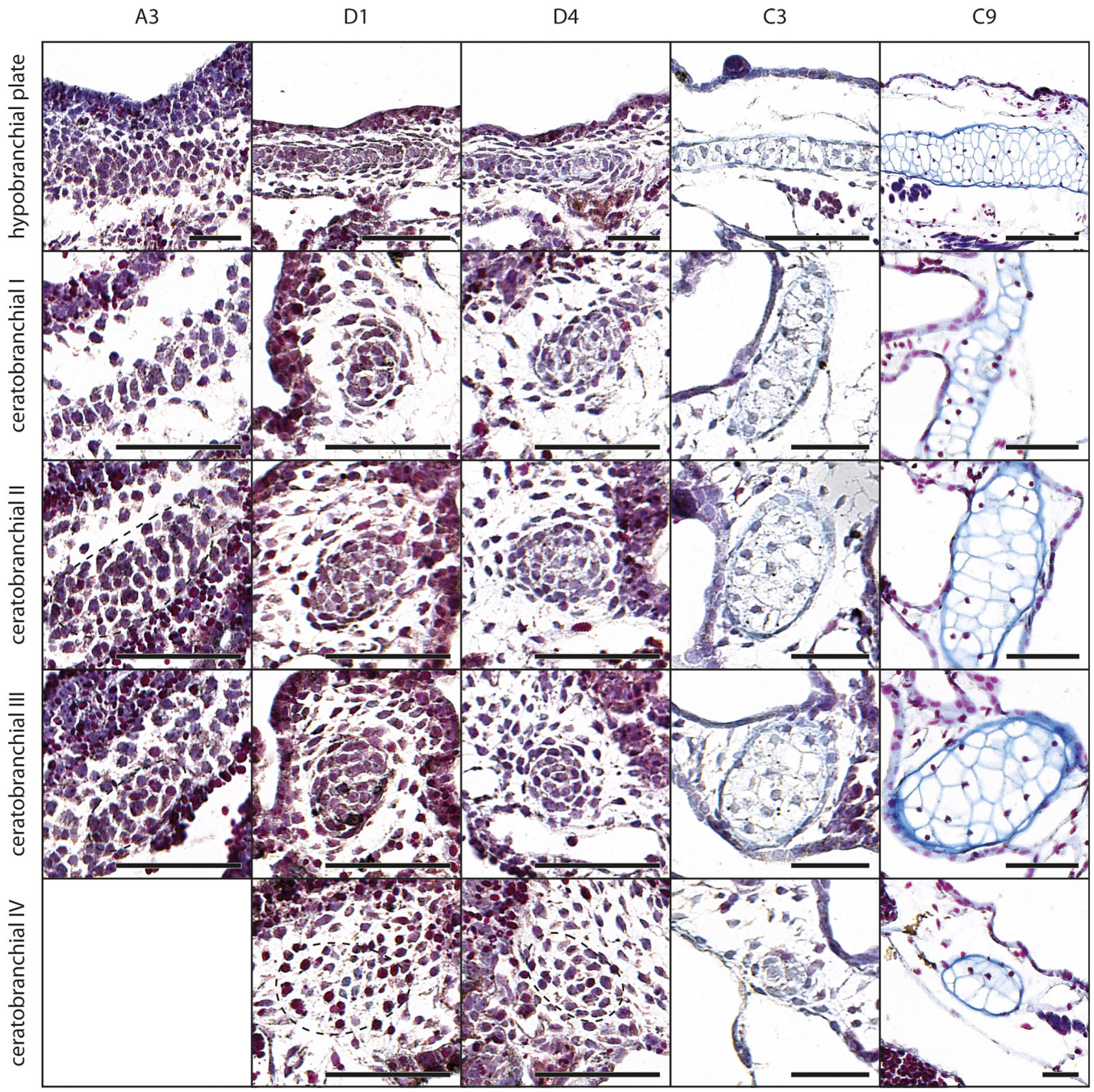

FIGURE 5 *Bufo bufo*, cartilaginous development of the branchial basket. Azan-stained, transverse histological sections of Stage A3 (first column), stage D1 (second column), stage D4 (third column), stage C3 (fourth column), and stage C9 (fifth column) show the chondrification process of the hypobranchial plate, and the ceratobranchials I-IV. Difficult observable structures are highlighted by dashed lines. Missing depictions indicate that no observable Anlagen were present. Relative position of the cross sections is shown in Figure 3c. Scale bars indicate 100 µm.

the ceratohyal moves. During the following stages the articular process of the palatoquadrate and its ascending process (C4) as well as the quadratoorbital commissure (C8) differentiate into proper cartilage (Figure 6). The mesenchymal Anlage of the quadratoethmoid process bulges at the anterior margin of the quadratocranial commissure at stage C4, differentiates into chondroblasts at stage C6, and chondrifies at stage C8.

3.5 | Ceratohyal

The ceratohyal of *B. bufo* is a paired cartilage which parts are connected via the pars reuniens. It consists of a corpus, an anterior, an anterolateral, a lateral, and a posterior process, as well as an articular condyle (Figure 1b). A postcondylar process, as commonly present in other anuran larvae, is not present. The ceratohyal develops from two

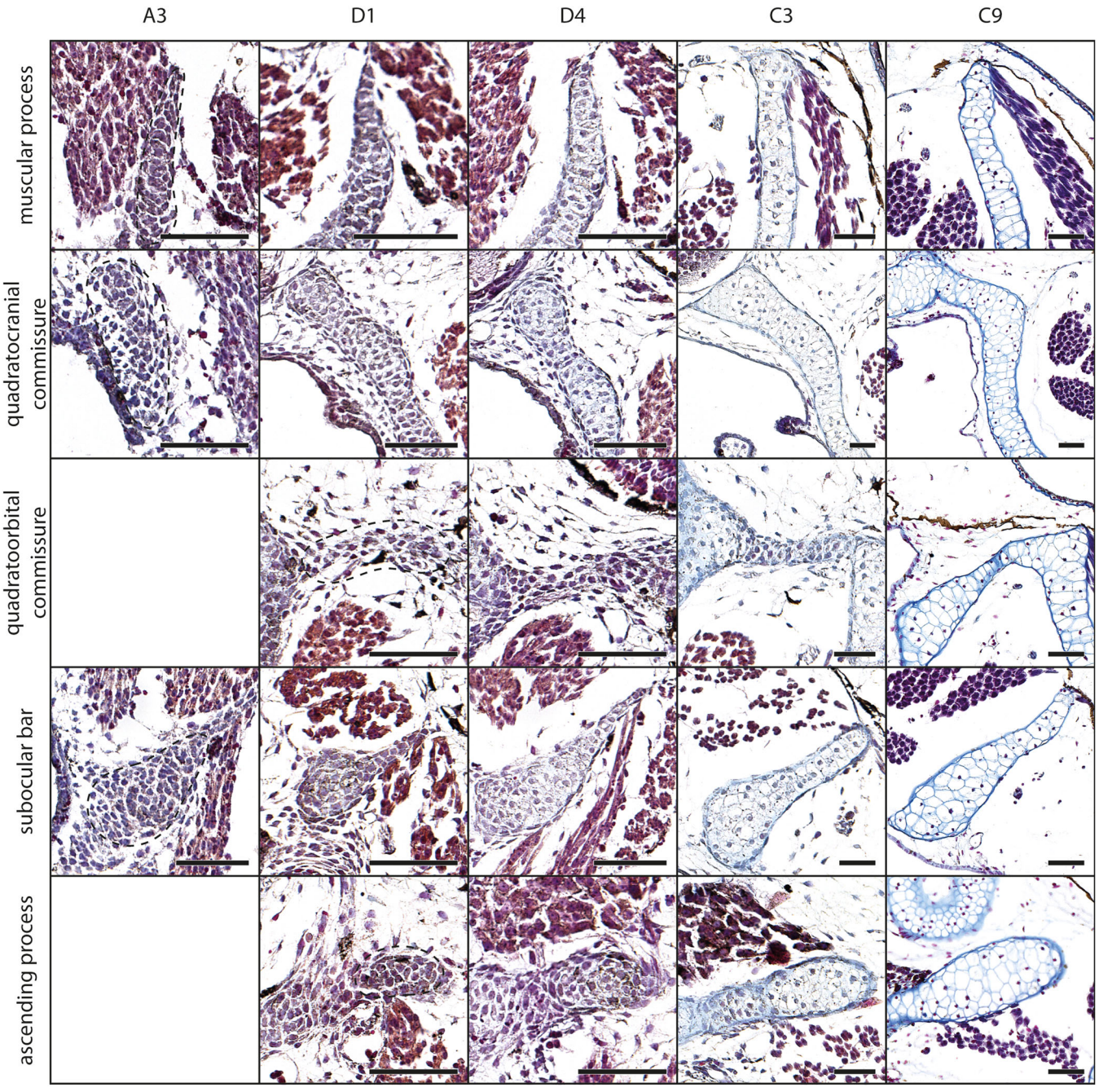

FIGURE 6 *Bufo bufo*, cartilaginous development of the palatoquadrate. Azan-stained, transverse histological sections of Stage A3 (first column), stage D1 (second column), stage D4 (third column), stage C3 (fourth column), and stage C9 (fifth column) show the chondrification process of the muscular process, the quadratocranial commissure, the quadratoorbital commissure, the subocular bar and the ascending process. Difficult observable structures are highlighted by dashed lines. Missing depictions indicate that no observable Anlagen were present. Relative position of the cross sections is shown in Figure 3d. Scale bars indicate 100 µm.

mesenchymal Anlagen ventral to the oral cavity and posterior to the Anlagen of Meckel's cartilage. The lateral process is bordered laterally by the Anlage of the M. orbitohyoideus. The mesenchymal Anlagen of the corpus, anterior, lateral, and posterior processes, and pars reuniens of the ceratohyal are present at stage A1. The posterior process of the ceratohyal is situated anteriorly to the Anlage of the hypobranchial plate. During further development the ceratohyal Anlage widens laterally and extends posteriorly. The posterior process becomes pointed. The articular condyle develops ventral to its counterpart, the hyoquadrate process of the palatoquadrate at stage A2. At stage D1 the cells of the corpus and the lateral process differentiate into chondroblasts followed by the anterior and posterior process at stage D2 (Figure 4). The articular condyle follows at stage D3. The lateral process begins to bend posteriorly. Its posterior tip borders the ceratobranchial I laterally. The anterior margin of the ceratohyal is curved until stage C1. Then the mesenchymal Anlage of the anterolateral process develops anteromedial

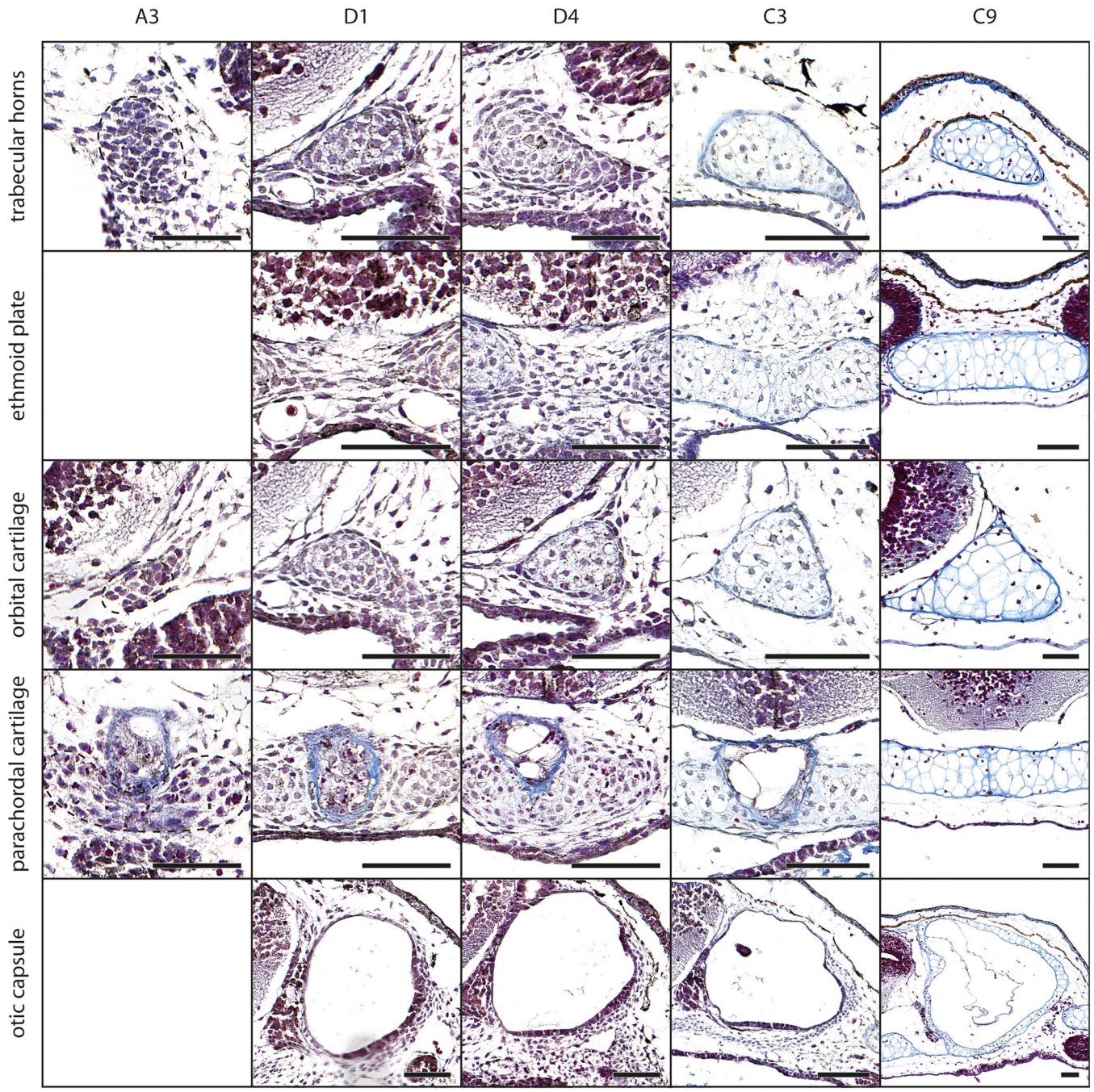

FIGURE 7 *Bufo bufo*, cartilaginous development of the neurocranium. Azan-stained, transverse histological sections of Stage A3 (first column), stage D1 (second column), stage D4 (third column), stage C3 (fourth column), and stage C9 (fifth column) show the chondrification process of the trabecular horns, the ethmoid plate, the orbital cartilage, the parachordal cartilage and the otic capsule. Difficult observable structures are highlighted by dashed lines. Missing depictions indicate that no observable Anlagen were present. Relative position of the cross sections is shown in Figure 3d. Scale bars indicate 100 µm.

to the articular condyle. The corpus and the anterior process consist of chondrocytes from this stage onwards. At stage C2 lateral and posterior processes also consist of chondrocytes, whereas the pars reuniens differentiates into chondroblasts and closes the median gap between the ceratohyals. Now only one Anlage is present. The last parts to chondrify are the articular condyle at stage C4, the pars reuniens at stage C6 and the anterolateral process at stage C8 (Figures 1b and 4).

3.6 | Basibranchial

The basibranchial is a cylindrical rod which narrows posteriorly. It is located between the ceratohyals and connected to the posterior surface of the pars reuniens (Figure 1b). It separates the anterior part of the hypobranchial plate. The posteroventral surface bears the urobranchial process, which is first clearly distinguishable but

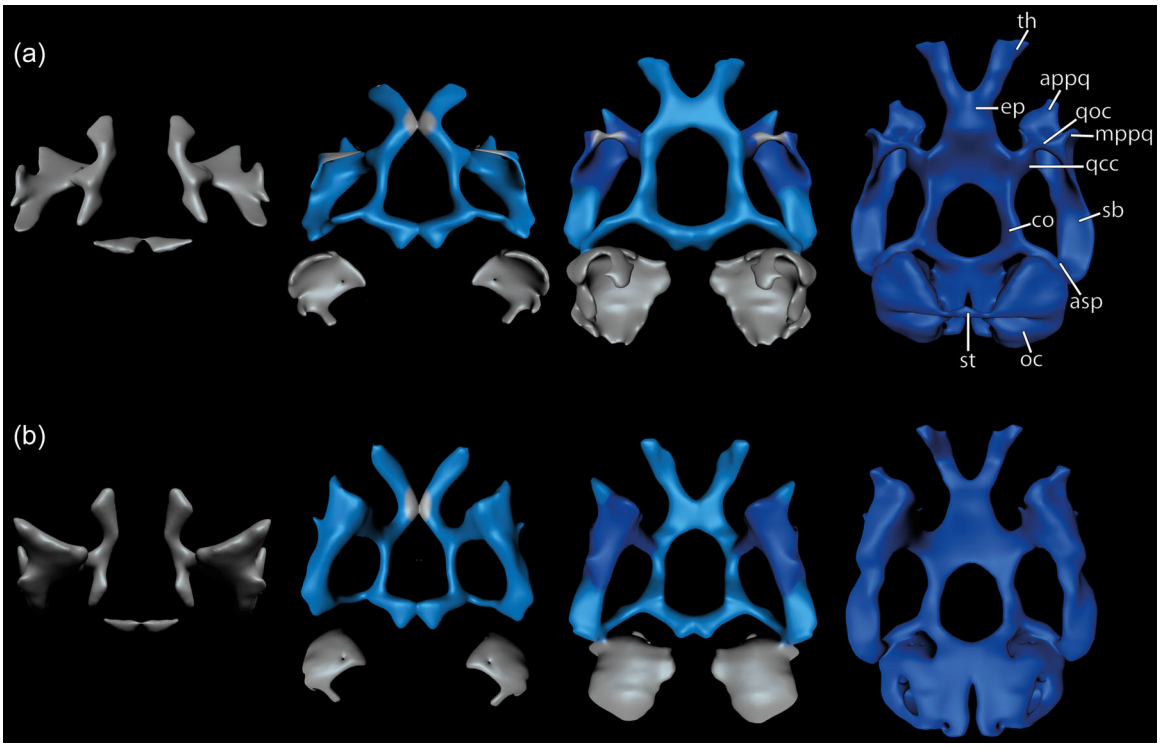

FIGURE 8 3D reconstructions of the head skeleton of larvae showing the cartilaginous development of palatoquadrate and the neurocranium during stages A3, D3, C1, and C9 (left to right) in dorsal (a) and ventral (b) view. The 3D reconstructions are color-coded, according to the distinct stage of cartilaginous development: "Light gray" means Anlagen are visible as mesenchymal cell clusters; "light blue" means that condensed precartilaginous cell clusters containing chondroblasts are visible, "dark blue" means that the respective cartilage contains chondrocytes rich in cytoplasm and bordered by a distinct perichondrium. Sizes were adjusted. appq, articular process of palatoquadrate; asp, ascending process; co, orbital cartilage; ep, ethmoid plate; mppq, muscular process of palatoquadrate; oc, otic capsule; qcc, quadratocranial commissure; qoc, quadratoorbital commissure; sb, subocular bar; st, synotic tectum; th, trabecular horn.

becomes more and more inconspicuous during further development. The mesenchymal Anlage of the basibranchial arises at stage A1 and is bordered laterally by the mesenchymal Anlage of the ceratohyal and posterolaterally by the mesenchymal Anlage of the hypobranchial plate. The Anlage is spherical and short, but extends posteriorly during further development. At stage A2 the short mesenchymal Anlage of the urobranchial process develops at the posteroventral surface. The Anlage of the basibranchial consists of chondroblasts at stage D3 and the anterior margin is now connected to the pars reuniens of the ceratohyal (Figure 1b). The urobranchial process differentiates into chondroblasts at stage C1. The precartilaginous Anlage becomes narrower but elongates posteriorly. The urobranchial process is pointed. The chondroblasts of both the basibranchial and the urobranchial process differentiate relatively late into chondroblasts at stage C7 and C8, respectively.

3.7 | Branchial basket

The branchial basket of *B. bufo* consists of a median hypobranchial plate, four ceratobranchials on each side which are connected laterally to each other via the terminal commissures I–III, and three spicules which emerge from the dorsolateral surface of the hypobranchial plate (Figure 1c). All three proximal commissures are missing in the investigated stages of *B. bufo*, therefore only ceratobranchial I is connected to the hypobranchial plate. Craniobranchial commissures and hypobranchials are also not present. The mesenchymal Anlage of the hypobranchial plate and ceratobranchial I and II develop at stage A1. The Anlage of the hypobranchial plate is beneath the posteroventral surface of the pharyngeal cavity. It is connected to the mesenchymal Anlage of ceratobranchial I, which develops beneath the posterolateral surface of the pharyngeal cavity. The mesenchymal Anlage of ceratobranchial II develops posterior to the mesenchymal Anlage of ceratobranchial I and also borders the posterolateral surface of the pharyngeal cavity. During further devlopment the mesenchymal Anlagen of ceratobranchial III (stage A2) and ceratobranchial IV (stage D1) arise in parallel to the Anlagen of the other ceratobranchials. All ceratobranchials further extend laterally and bend posterolaterally. Ceratobranchials II–IV are not connected to other cartilaginous Anlagen. Their medial tips extend close to the hypobranchial plate, but do not fuse with it. The lateral tips of all ceratobranchial bend posteriorly but a gap between neighboring ceratobranchials still remains until stage D1 when the mesenchymal Anlage of the terminal commissure I arises and connects the distal tips of ceratobranchial I and II. At stage D2 a small outgrowth appears at the mediodorsal surface of

ceratobranchial I, which is the mesenchymal Anlage of spicule I. From stage D3 onwards the mesenchymal Anlage of the terminal commissure II connects the distal tips of ceratobranchial II and III (Figure 1c). The mesenchymal Anlage of ceratobranchial II is the first to differentiate into chondroblasts at stage D2, followed by ceratobranchial I and the hypobranchial plate at stage D4. The mesenchymal Anlage of spicule II arises at the lateral surface of the hypobranchial plate. At stage C1 the Anlage of ceratobranchial III consists of chondroblasts and the mesenchymal Anlage of spicule III appears at the posterolateral surface of the hypobranchial plate (Figure 1c). The mediodorsal surface of ceratobranchial I bulges anteriorly. All cartilaginous elements of the branchial basket are connected from stage C2 onwards because the last part, the mesenchymal Anlage of the terminal commissure III, develops between the lateral tips of ceratobranchials III and IV. The hypobranchial plate consists of chondroblasts at this stage and is, therefore, the first element of the branchial basket to start the chondrification process. It further elongates posteriorly and remains plate-like. Ceratobranchial I chondrifies at stage C3 (Figure 5), followed by terminal commissure I, and ceratobranchial II at stage C4 and ceratobranchial III at stage C6. Spicule I, terminal commissure II, and ceratobranchial IV chondrify at stage C7, and the remaining spicules II-III and terminal commissure III chondrify between the stages C8 and C9 (Figures 1c and 5). The general shape of the branchial basket is acquired at stage C8 and it only widens posteriorly and laterally which results in slender ceratobranchials and a more filigreed appearance.

3.8 | Neurocranium

The neurocranium of *B. bufo* consists of paired trabecular horns, a single ethmoid plate bordering the brain anteriorly, a basicranial floor bordering the brain ventrally, and a synotic tectum connecting the otic capsules dorsally. Bilaterally present are an antorbital process, an orbital cartilage flanking the brain laterally and the eye medially, a quadratoethmoid process, a parachordal cartilage flanking the notochord, and an otic capsule which surrounds the inner ear (Figure 8). The development of the neurocranium starts at stage A1 with the two anteriormost elements. Two spherical mesenchymal Anlagen of the trabecular horns are present which surround the pharyngeal cavity anterodorsally. The mesenchymal Anlage of the orbital cartilage appears posterior to the Anlage of the trabecular horn and is not connected to it. The anterior part of the trabecular horn bends ventrally and the posterior part elongates posteriorly during further development. The Anlage of the orbital cartilage also extends posteriorly. At stage A3 the two mesenchymal Anlagen of the parachordal cartilage appear on both sides of the anterior tip of the notochord (Figures 8 and 7). The lateral part of the otic capsule becomes visible as a mesenchymal Anlage at stage A4. The posterior part of the trabecular horns is connected by the mesenchymal Anlage of the ethmoid plate at stage D1 (Figure 7). At the same stage the Anlagen of the trabecular horn and the orbital cartilage consist of chondroblasts. The Anlagen of the parachordals fuse at stage D1 and the cells also differentiates into chondroblasts (Figure 8). The parachordal further elongates posteriorly flanking the developing otic capsule medially. The ethmoid plate widens and consists of chondroblasts at stage C1 (Figure 8). The first structures of the neurocranium to chondrify are the trabecular horns and the orbital cartilage at stage C2, followed by the ethmoid plate and the parachordal cartilage at stage C3 (Figure 7). At stage C4 the lateral part of the otic capsule differentiates into chondroblasts. Differentiation continues in the medial direction during stages C4–C6. At stage C7 the antorbital process emerges at the anterodorsal part of the orbital cartilage. At the same stage the lateral part of the otic capsule differentiates into chondrocytes and once again this differentiation continues in the medial direction. A small band of mesenchymal cells connects the dorsal part of both otic capsules at stage C7. This Anlage of the synotic tectum becomes precartilaginous at stage C8 and chondrifies at stage C9. At the same time the basicranial floor develops first at the lateral margin of the basicranial fenestra (stage C7). During further development the basicranial floor closes the fenestra and develops into a cartilaginous plate which encapsulates the brain anteroventrally (stage C10). The posterior part of the basicranial fenestra is still present at this stage but shrinks during further development.

4 | DISCUSSION

The present study describes the chondrogenesis of all major cartilaginous components of the larval head skeleton of *B. bufo*. The major steps of cartilaginous development of *B. bufo* take place between Go21 and Go28. As stated for *Bombina orientalis* and *Xenopus laevis* the process of skeletal development does not correspond to the external development (Lukas & Olsson, 2018, 2020). Therefore, the internal sequence of cartilaginous development can not be determined by external developmental characters due to the variation in the timing of both. 18 substages are presented, where each substage is defined by a specific combination of the presence or absence of different cartilages at different developmental states.

4.1 | Developmental sequence of chondrogenesis

It has been shown that the appearance of Anlagen and the chondrification of the viscerocranial derivatives in chondrichthyans (Gillis et al., 2009, 2012), teleosts (Langille & Hall, 1987), and sturgeons (Warth et al., 2017) follows a strict anterior to posterior direction. At least the two basal anurans *Bombina orientalis* and *Xenopus laevis*, which have been investigated do not conform to this ancient pattern. The mesenchymal Anlagen of the ceratohyal, a derivative of the hyoid arch, appear before the Anlagen of the derivatives of the mandibular arch like the infrarostral cartilage or

Meckel's cartilage (Lukas & Olsson, 2018, 2020). Additionally, the ceratohyal chondrifies before the mandibular arch derivatives. *Discoglossus scovazzi*, which is closely related to *Bombina orientalis* partially follows the ancient anterior to posterior pattern because at least some derivatives of the mandibular arch chondrify before the ceratohyal (Lukas & Ziermann, 2022). The initial assumption, that the early development of the ceratohyal might be linked to its importance as the central element of the buccal pump and that its early development might be an apomorphic trait for the Lalagobatrachia (Lukas & Olsson, 2020) is challenged by this finding. *B. bufo* differs from both sequences, because some derivatives of the mandibular and the hyoid arch (ceratohyal, quadratocranial commissure, muscular process of the palatoquadrate) chondrify simultaneously. The developmental sequence of the ceratohyal in *B. bufo* also follows a pattern observed in *Xenopus laevis* and *Bombina orientalis*. In all three species the ceratohyal is the first observable mesenchymal Anlage, the first Anlage which differentiates into chondroblasts and the first to chondrify during development. The problem can not be fully resolved with the present data but the results from *B. bufo* might shift the view to the following scenario: The mesenchymal Anlage of the ceratohyal corpus is the first one which appears during development, and it is the first one which chondrifies in *Bombina orientalis*, *Xenopus laevis*, and *B. bufo*. This is supposed to be an apomorphic trait and ontogenetic novelty of the Lalagobatrachia, while lost secondarily in *Discoglossus scovazzi* (Figure 9).

The chondrification of the viscerocranial derivatives of *B. bufo* is mosaic-like instead of a straightforward in an anterior to posterior sequence. The development of the infrarostral cartilage of *B. bufo*, a derivative of the mandibular arch, lags behind the development of the ceratohyal, hypobranchial plate, ceratobranchial I, and ceratobranchial II. Regarding the infrarostral cartilage of *B. bufo*, all three described major steps of chondrocranial development (mesenchymal Anlage,

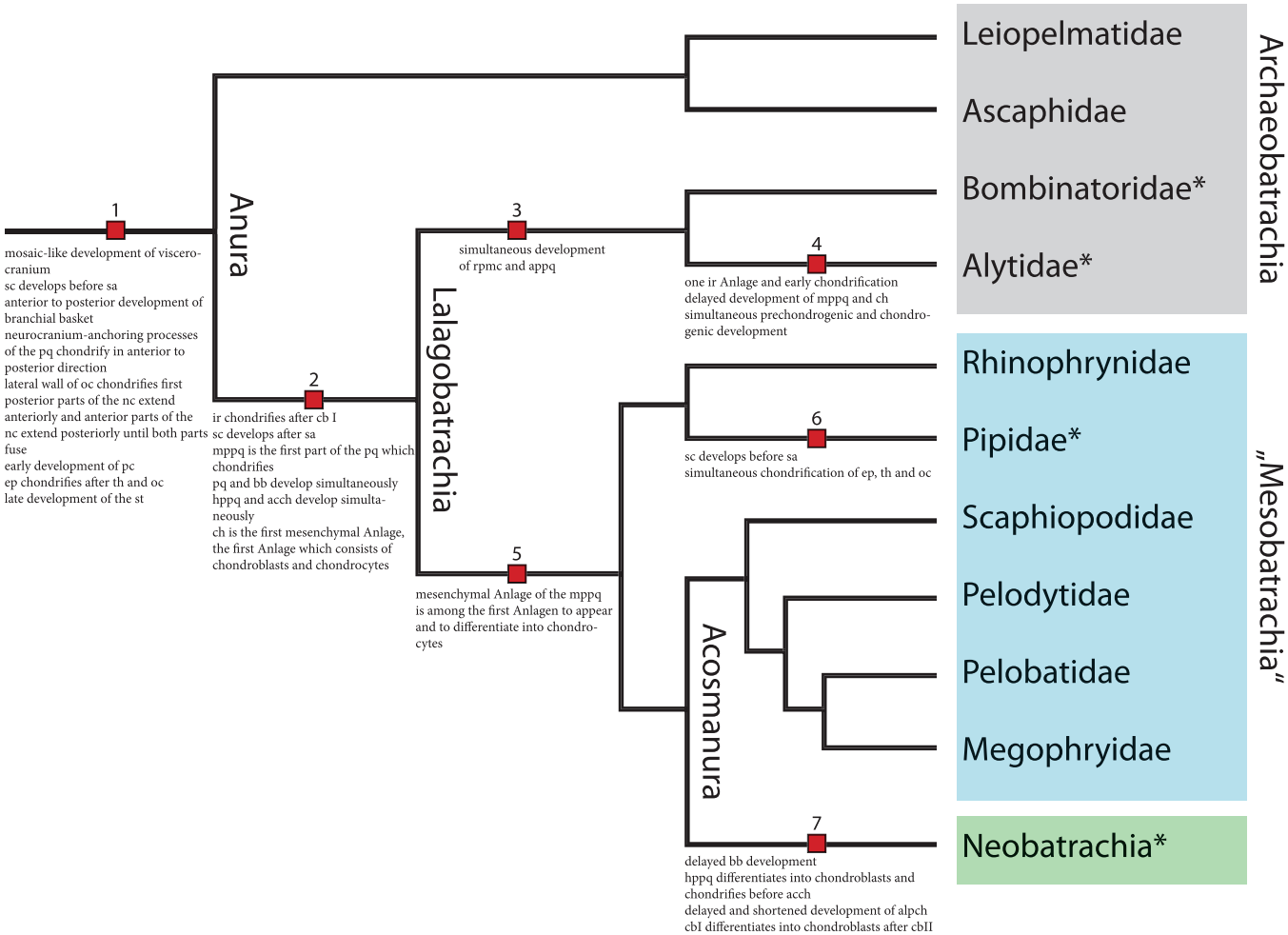

FIGURE 9 Cladogram of extant anurans with mapped features of cartilaginous development which underline the relationships of anuran families. Asterisks mark the taxa where sequential information on the larval cartilaginous head development is available. This information is the basis for the hypothesized features (for details see Section 4). acch, articular condyle of ceratohyal; alpch, anterolateral process of ceratohyal; appq, articular process of palatoquadrate; bb, basibranchial; cb I–II, ceratobranchial I–II; ch, ceratohyal; ep, ethmoid plate; hppq, hyoquadrate process of palatoquadrate; ir, infrarostral cartilage; mppq, muscular process of palatoquadrate; nc, neurocranium; oc, otic capsule; pc, parachordal cartilage; pq, palatoquadrate; rpmc, retroarticular process of Meckel's cartilage; sa, suprarostral ala; sc, suprarostral corpus; th, trabecular horn.

differentiation into chondroblasts and chondrification) are observed later than in the ceratohyal, hypobranchial plate, ceratobranchial I and ceratobranchial II, which are derivatives of the hyoid arch and the branchial arches I and II, respectively. Even the terminal commissure I chondrifies before the infrarostral cartilage. A similar pattern was observed in *Bombina orientalis* and *Xenopus laevis*. In the latter also ceratobranchial III and ceratobranchial IV chondrify before the infrarostral cartilage. Ceratobranchials I–IV have been reported to develop stepwise in anterior to posterior direction in *B. orientalis*, *X. laevis*, *Rana temporaria*, *Bufo cinereus*, and *Hyla sp*. but less stepwise and more simultaneous in *Discoglossus scovazzi* (Lukas & Olsson, 2018, 2020; Lukas & Ziermann, 2022; Parker, 1871; Stöhr, 1882). Ceratobranchials I and II have an almost simultaneous pattern of development in *B. orientalis*, *X. laevis*, and *D.s scovazzi* with the only difference that ceratobranchial II chondrifies one stage after ceratobranchial I. Mesenchymal Anlagen and chondroblasts appear at the same stages in all three species. In *B. bufo* both mesenchymal Anlagen arise at the same stage but ceratobranchial II differentiates two stages before ceratobranchial I. Nevertheless, ceratobranchial I chondrifies one stage before ceratobranchial II. The development of spicules I–III and terminal commissures I–III follows the strict anterior to posterior pattern observed before. Further investigations on the larval cartilaginous development should clarify if the change of the strict anterior to posterior sequence of chondrification within the branchial basket is an exception or an evolutionary trend based on heterochronic shifts or evolutionary changes of the developmental sequence (Figure 9).

Similarly to the infrarostral cartilage, the suprarostral cartilage is an apomorphic trait of anurans. Except in *D. scovazzi*, the suprarostral cartilage develops after the palatoquadrate, Meckel's cartilage, ceratohyal and the trabecular horns in the anuran larvae investigated so far (Lukas & Olsson, 2018, 2020; Lukas & Ziermann, 2022; Stöhr, 1882), thus breaking the anterior to posterior pattern. In *B. bufo*, the establishment of the mesenchymal Anlagen, the differentiation into chondroblasts, and chondrification of the suprarostral alae takes place earlier than in the suprarostral corpus. The same pattern was observed in *B. orientalis* and *D. scovazzi* (Lukas & Olsson, 2020; Lukas & Ziermann, 2022) but not in *X. laevis*, where the suprarostral is a plate fused to the trabecular horns, (Lukas & Olsson, 2018), and neither in *Ascaphus truei* (Reiss, 1997). In both species, the lateral parts of the suprarostral develop later than the medial. This raises the question of the ancestral sequence of suprarostral development.

Four possible scenarios for the ancestral sequence of suprarostral development have been presented before. Based on the present results I can update these scenarios as follows. (1) The medial first and lateral second sequence of *Ascaphus truei* is an apomorphic trait of all anurans. The lateral first and medial second sequence has evolved at least twice independently in Discoglossoids and Bufonids. (2) The medial first and lateral second sequence is an apomorphic trait of all anurans. The lateral first and medial second sequence is a derived trait of the Lalagobatrachia but it was lost secondarily in Pipoids. (3) The lateral first and medial second sequence is an apomorphic trait of all anurans. The medial first and lateral second sequence has evolved at least twice independently in Ascaphids and Pipoids. (4) The lateral first and medial second sequence is plesiomorphic for Discoglossoids and Bufonids and the medial first and lateral second sequence is plesiomorphic for Ascaphids and Pipoids. The ancestral sequence is different.

It has been shown in several gnathostomes, that Meckel's cartilage and the palatoquadrate, the derivatives of the mandibular arch, originate from a single Anlage (Cerny et al., 2004; Gillis et al., 2009). The mesenchymal Anlage splits into a ventral part, which gives rise to Meckel's cartilage and a lateral part, which gives rise to the palatoquadrate. After separation both cartilages develop independently. In recently investigated anurans as well as in the present study of *B. bufo*, two separate Anlagen of Meckel's cartilage and palatoquadrate are observable in the earliest specimens investigated (Lukas & Olsson, 2018, 2020; Lukas & Ziermann, 2022; Stöhr, 1882). If a single Anlage was present earlier can not be excluded with the present data. The retroarticular process of Meckel's cartilage chondrifies after its corresponding part of the palatoquadrate, the articular process in *B. bufo*, but In *X. laevis* it chondrifies before the articular process (Lukas & Olsson, 2018). The development of both processes which establish the primary jaw joint proceeds simultaneously in *B. orientalis* and *D. scovazzi* (Lukas & Olsson, 2020; Lukas & Ziermann, 2022). This would support the scenario that the sequence of development is much more flexible than assumed as long as the resulting structures are functional (Ziermann et al., 2014). This simultaneous development might be a shared feature of Discoglossoids (Figure 9). The variability of the timing between both processes in different taxa needs further attention in future investigations to identify possible evolutionary changes or heterochronic shifts.

The muscular process of the palatoquadrate is the first part of the palatoquadrate which chondrifies in *B. orientalis*, *X. laevis*, and *B. bufo* (Lukas & Olsson, 2018, 2020). In *D. scovazzi* the quadratocranial commissure chondrifies before the muscular process (Lukas & Ziermann, 2022). Thus, the muscular process being the first part of the palatoquadrate to chondrify, might be a shared feature of Lalagobatrachians while secondarily lost in *Discoglossus* (Figure 9). Additionally, the mesenchymal Anlage of the muscular process is among the first Anlagen to appear and among the first to differentiate into chondrocytes in Xenoanura and Acosmanura so far. However, significantly more species should be studied to make more concrete assumptions about additional apomorphic or plesiomorphic developmental traits.

The mesenchymal Anlagen of the hyoquadrate process of the palatoquadrate and the articular condyle of the ceratohyal arise at the same stage in *D. scovazzi*, *B. orientalis*, *X. laevis*, and *B. bufo* (Lukas & Olsson, 2018, 2020; Lukas & Ziermann, 2022). The Anlagen differentiate into chondroblasts and chondrify simultaneously in *Discoglossus scovazzi*. In *B. orientalis* and *X. laevis* the articular condyle consists of chondroblasts and chondrifies before the hyoquadrate process (Lukas & Olsson, 2018, 2020). However, in *B. bufo* the hyoquadrate process differentiates into chondroblasts and chondrifies before the articular condyle. The almost simultaneous development of the hyoquadrate process and the articular condyle may be an

ancestral feature while the forward displacement of the hyoquadrate process may be a derived feature of Neobatrachians (Figure 9). Once again further research on additional species should shed light on this question. In *B. orientalis*, the mesenchymal Anlage of the anterolateral process of the ceratohyal develops when the first cartilages differentiate into chondroblasts while it develops in *B. bufo* not until the first cartilages chondrify. This late and short development of the anterolateral process in *B. bufo* differs greatly from the extended and early development in *B. orientalis*. The development of the anterolateral process needs to be investigated in further anuran species to identify a possible evolutionary trend.

Investigations on several Osteichthyes, including Japanese medaka (Langille & Hall, 1987), sturgeons (Warth et al., 2017), coelacanth (Dutel et al., 2019), Australian lungfish (Kemp, 1999), "reptiles" (De Beer, 1937; Gaupp, 1904; Hernández-Jaimes et al., 2012; Ollonen et al., 2018; Tulenko & Sheil, 2007), and birds (Hüppi et al., 2021), have observed a posterior to anterior direction of neurocranium development. In the species investigated the otic capsules, parachordals, and cranial trabeculae, are all posterior parts of the neurocranium, and are the first cartilages which develop during chondrogenesis. Once these posterior parts are established, they grow anteriorly to form the neurocranium. Anurans investigated so far differ from this osteichthyan pattern (Lukas & Ziermann, 2022) and the results from *B. bufo* further support this. In the basal anuran *Ascaphus truei* and the more derived *D. scovazzi* the parachordal cartilage is the first or among the first cartilages to chondrify, respectively (Lukas & Ziermann, 2022; Reiss, 1997). In other investigated anurans the chondrification of this cartilage is delayed. The same goes for the otic capsule, whose development is even more delayed. Additionally, it always chondrifies on its lateral wall first (lateral to medial direction) (Lukas & Olsson, 2018, 2020; Lukas & Ziermann, 2022; Reiss, 1997; Stöhr, 1882). The posterior parts of the neurocranium like the parachordals extend anteriorly, while the anterior parts of the neurocranium, the trabecular horns and the orbital cartilage, extend posteriorly until both parts meet and fuse at the midline. This clearly differs from the gnathostomian posterior to anterior pattern (Figure 9). In anurans, the ethmoid plate chondrifies after the trabecular horns and the orbital cartilages. One exception is *X. laevis* where they chondrify simultaneously. This could be a derived feature of *X. laevis* because of the incorporation of the ethmoid plate and the trabecular horns into the suprarostral plate. The late development of the synotic tectum, which is a common feature of anurans but also present in avians and Australian lungfish, was observed in *B. bufo* too and further confirms this pattern (Hüppi et al., 2021; Kemp, 1999; Lukas & Olsson, 2018, 2020; Lukas & Ziermann, 2022; Reiss, 1997; Stöhr, 1882).

5 | CONCLUSIONS

The timing of the cranial chondrification of three basal anuran species and one neobatrachian species was thoroughly compared. I can confirm that the posterior to anterior growth of the parachordal and the initial development of the lateral wall of the otic capsule are shared gnathostome features. Nevertheless, all anurans studied so far differ in several features from the ancestral pattern. The viscerocranial structures do not chondrify in a strict anterior to posterior pattern. Instead, the viscerocranial development is stepwise and mosaic-like. This mosaic-like development may be caused by the evolution of several novel cartilages within the mandibular arch including the suprarostral, infrarostral, adrostral, and admandibular cartilages. The development of these unique cartilages is clearly delayed after the development of hyoid and branchial arch derivatives. Nevertheless, strict anterior to posterior patterns can be observed within the development of the branchial basket. Another gnathostome feature is the posterior to anterior development of the neurocranium. Once again, anurans differ greatly from this pattern because neurocranial elements do not develop in strict posterior to anterior direction. Instead, the posterior elements extend anteriorly and the anterior elements extend posteriorly until both parts meet at the midline. Additionally, I propose several features, which underline the relationship of several taxa within the anuran clade (Figure 9). These proposed features are a good basis to test hypotheses regarding developmental sequences and their evolution in upcoming studies with the inclusion of more species.

ACKNOWLEDGEMENTS

The author is very grateful to Katja Felbel for technical support and preparation of the histological sections and to Patricia Kramarz for the preparation of the cleared and stained specimens. I thank Lennart Olsson for the critical revision of an early version of the manuscript. I also gratefully acknowledge the positive input made by Janine Ziermann and one anonymous reviewer on earlier manuscript versions. PL is supported by a grant from the German Research Foundation (grant number: LU 2404/1-1). Open Access funding enabled and organized by Projekt DEAL.

DATA AVAILABILITY STATEMENT

The data that support the findings of this study are available from the corresponding author upon reasonable request.

ORCID

Paul Lukas http://orcid.org/0000-0003-2756-0465

PEER REVIEW

The peer review history for this article is available at https://www.webofscience.com/api/gateway/wos/peer-review/10.1002/jez.b.23214.

REFERENCES

Angel, F., & Lamotte, M. (1944). Un crapaud vivipare d'Afrique Occidentale (*Nectophrynoides occidentalis* Angel). *Annales des Sciences Naturelles, Zoologie*, *6*, 63–89.

De Beer, G. R. (1937). *The development on the vertebrate skull*. Oxford University Press.

Bonacci, A., Brunelli, E., Sperone, E., & Tripepi, S. (2008). The oral apparatus of tadpoles of *Rana dalmatina*, *Bombina variegata*, *Bufo*

bufo, and *Bufo viridis* (Anura). *Zoologischer Anzeiger - A Journal of Comparative Zoology*, *247*(1), 47–54. https://doi.org/10.1016/j.jcz.2007.02.004

Cardona, A., Saalfeld, S., Schindelin, J., Arganda-Carreras, I., Preibisch, S., Longair, M., Tomancak, P., Hartenstein, V., & Douglas, R. J. (2012). TrakEM2 software for neural circuit reconstruction. *PLoS One*, *7*(6), e38011. https://doi.org/10.1371/journal.pone.0038011

Cerny, R., Lwigale, P., Ericsson, R., Meulemans, D., Epperlein, H. H., & Bronner-Fraser, M. (2004). Developmental origins and evolution of jaws: New interpretation of "maxillary" and "mandibular". *Developmental Biology*, *276*(1), 225–236. https://doi.org/10.1016/j.ydbio.2004.08.046

Cerny, R., Horáček, I., & Olsson, L. (2006). The trabecula cranii: Development and homology of an enigmatic vertebrate head structure. *Animal Biology*, *56*, 503–518. https://doi.org/10.1163/157075606778967801

Couly, G. F., Coltey, P. M., & le Douarin, N. M. (1992). The developmental fate of the cephalic mesoderm in quail-chick chimeras. *Development*, *114*, 1–15. https://doi.org/10.1242/dev.114.1.1

Depew, M. J., Lufkin, T., & Rubenstein, J. L. R. (2002). Specification of jaw subdivisions by Dlx genes. *Science*, *298*(5592), 381–385. https://doi.org/10.1126/science.10757

Diaz-Paniagua, C. (1989). Larval diets of two anuran species, *Pelodytes punctatus* and *Bufo bufo*, in SW Spain. *Amphibia-Reptilia*, *10*(1), 71–75. https://doi.org/10.1163/156853889X00304

Dingerkus, G., & Uhler, L. D. (1977). Enzyme clearing of alcian blue stained whole small vertebrates for demonstration of cartilage. *Stain Technology*, *52*(4), 229–232. https://doi.org/10.3109/10520297709116780

Dutel, H., Galland, M., Tafforeau, P., Long, J. A., Fagan, M. J., Janvier, P., Herrel, A., Santin, M. D., Clément, G., & Herbin, M. (2019). Neurocranial development of the coelacanth and the evolution of the sarcopterygian head. *Nature*, *569*(7757), 556–559. https://doi.org/10.1038/s41586-019-1117-3

Franz-Odendaal, T. A., Hall, B. K., & Witten, P. E. (2006). Buried alive: How osteoblasts become osteocytes. *Developmental Dynamics*, *235*, 176–190. https://doi.org/10.1002/dvdy.20603

Frost, D. R., Grant, T., Faivovich, J., Bain, R. H., Haas, A., Haddad, C. F. B., DE SÁ, R. O., Channing, A., Wilkinson, M., Donnellan, S. C., Raxworthy, C. J., Campbell, J. A., Blotto, B. L., Moler, P., Drewes, R. C., Nussbaum, R. A., Lynch, J. D., Green, D. M., & Wheeler, W. C. (2006). The amphibian tree of life. *Bulletin of the American Museum of Natural History*, *297*, 1–291. https://doi.org/10.1206/0003-0090(2006)297[0001:TATOL]2.0.CO;2

Gaupp, E. (1904). *Die Entwicklung des Kopfskelettes Handbuch der vergleichenden und experimentalen Entwickelungsgeschichte der Wirbeltiere*. Fischer.

Gillis, J. A., Dahn, R. D., & Shubin, N. H. (2009). Chondrogenesis and homology of the visceral skeleton in the little skate, *Leucoraja erinacea* (Chondrichthyes: Batoidea). *Journal of Morphology*, *270*(5), 628–643. https://doi.org/10.1002/jmor.10710

Gillis, J. A., Modrell, M. S., & Baker, C. V. H. (2012). A timeline of pharyngeal endoskeletal condensation and differentiation in the shark, *Scyliorhinus canicula*, and the paddlefish, *Polyodon spathula*. *Journal of Applied Ichthyology*, *28*(3), 341–345. https://doi.org/10.1111/j.1439-0426.2012.01976.x

Goldring, M. B., Tsuchimochi, K., & Ijiri, K. (2006). The control of chondrogenesis. *Journal of Cellular Biochemistry*, *97*, 33–44. https://doi.org/10.1002/jcb.20652

Gosner, K. L. (1960). A simplified table for staging anuran embryos larvae with notes on identification. *Herpetologists' League*, *16*, 183–190.

Gross, J. B., & Hanken, J. (2008). Segmentation of the vertebrate skull: Neural-crest derivation of adult cartilages in the clawed frog, *Xenopus laevis*. *Integrative and comparative biology*, *48*(5), 681–696. https://doi.org/10.1093/icb/icn077

Haas, A. (2003). Phylogeny of frogs as inferred from primarily larval characters (Amphibia: Anura). *Cladistics*, *19*(1), 23–89. https://doi.org/10.1111/j.1096-0031.2003.tb00405.x

Hall, B. K., & Miyake, T. (1995). Divide, accumulate, differentiate: Cell condensation in skeletal development revisited. *The International Journal of Developmental Biology*, *39*, 881–893.

Hall, B. K., & Miyake, T. (2000). All for one and one for all: Condensations and the initiation of skeletal development. *BioEssays*, *22*, 138–147. https://doi.org/10.1002/(SICI)1521-1878(200002)22:2<138::AID-BIES5>3.0.CO;2-4

Handrigan, G. R., & Wassersug, R. J. (2007). The anuran Bauplan: A review of the adaptive, developmental, and genetic underpinnings of frog and tadpole morphology. *Biological Reviews*, *82*, 1–25. https://doi.org/10.1111/j.1469-185X.2006.00001.x

Harrington, S. M., Harrison, L. B., & Sheil, C. A. (2013). Ossification sequence heterochrony among amphibians. *Evolution & Development*, *15*(5), 344–364. https://doi.org/10.1111/ede.12043

Heidenhain, M. (1915). Uber die mallorysche bindegewebsfarbjung mit karmin und azokarmin als vorfarben. *Zeitschrift für wissenschaftliche Mikroskopie und für mikroskopische Technik*, *32*, 361–372.

Hernández-Jaimes, C., Jerez, A., & Ramírez-Pinilla, M. P. (2012). Embryonic development of the skull of the Andean lizard *Ptychoglossus bicolor* (Squamata, Gymnophthalmidae). *Journal of Anatomy*, *221*(4), 285–302. https://doi.org/10.1111/j.1469-7580.2012.01549.x

Hüppi, E., Werneburg, I., & Sánchez-Villagra, M. R. (2021). Evolution and development of the bird chondrocranium. *Frontiers in zoology*, *18*(1), 21. https://doi.org/10.1186/s12983-021-00406-z

Kemp, A. (1999). Ontogeny of the skull of the Australian lungfish *Neoceratodus forsteri* (Osteichthyes: Dipnoi). *Journal of Zoology*, *248*(1), 97–137. https://doi.org/10.1111/j.1469-7998.1999.tb01027.x

Kuratani, S., Matsuo, I., & Aizawa, S. (1997). Developmental patterning and evolution of the mammalian viscerocranium: Genetic insights into comparative morphology. *Developmental Dynamics*, *209*(2), 139–155. https://doi.org/10.1002/(SICI)1097-0177(199706)209:2<139::AID-AJA1>3.0.CO;2-J

Kuratani, S. (1999). Development of the chondrocranium of the loggerhead turtle, *Caretta caretta*. *Zoological Science*, *16*(5), 803–818. https://doi.org/10.2108/zsj.16.803

Kuratani, S. (2012). Evolution of the vertebrate jaw from developmental perspectives. *Evolution & Development*, *14*(1), 76–92. https://doi.org/10.1111/j.1525-142X.2011.00523.x

Langille, R. M., & Hall, B. K. (1987). Development of the head skeleton of the Japanese medaka, *Oryzias latipes* (Teleostei). *Journal of Morphology*, *193*(2), 135–158. https://doi.org/10.1002/jmor.1051930203

Lukas, P., & Olsson, L. (2018). Sequence and timing of early cranial skeletal development in *Xenopus laevis*. *Journal of Morphology*, *279*(1), 62–74. https://doi.org/10.1002/jmor.20754

Lukas, P., & Olsson, L. (2020). Sequence of chondrocranial development in the oriental fire bellied toad *Bombina orientalis*. *Journal of Morphology*, *281*(6), 688–701. https://doi.org/10.1002/jmor.21138

Lukas, P., & Ziermann, J. M. (2022). Sequence of chondrocranial development in basal anurans—Let's make a cranium. *Frontiers in zoology*, *19*(1), 17. https://doi.org/10.1186/s12983-022-00462-z

McDiarmid, R. W., & Altig, R. (1999). *Tadpoles: The biology of anuran larvae*. University of Chicago Press.

Ollonen, J., Da Silva, F. O., Mahlow, K., & Di-Poï, N. (2018). Skull development, ossification pattern, and adult shape in the emerging lizard model organism *Pogona vitticeps*: A comparative analysis with other squamates. *Frontiers in Physiology*, *9*(278), 1–26. https://doi.org/10.3389/fphys.2018.00278

Olsson, L., & Hanken, J. (1996). Cranial neural-crest migration and chondrogenic fate in the oriental fire-bellied toad *Bombina orientalis*:

Defining the ancestral pattern of head development in anuran amphibians. *Journal of Morphology*, *229*, 105–120. https://doi.org/10.1002/(SICI)1097-4687(199607)229:1<105::AID-JMOR7>3.0.CO;2-2

Parker, W. K. (1871). On the structure and development of the skull of the common frog (*Rana temporaria*, L.). *Philosophical Transactions of the Royal Society of London*

Parker, W. K. (1876). XXIV. On the structure and development of the skull in the batrachia.—Part II. *Philosophical Transactions of the Royal Society of London*, *166*, 601–669.

Pyron, R. A. (2014). Biogeographic analysis reveals ancient continental vicariance and recent oceanic dispersal in amphibians. *Systematic Biology*, *63*, 779–797. https://doi.org/10.1093/sysbio/syu042

Reiss, J. O. (1997). Early development of chondrocranium in the tailed frog *Ascaphus truei* (Amphibia: Anura): implications for anuran palatoquadrate homologies. *Journal of Morphology*, *231*(1), 63–100. https://doi.org/10.1002/(SICI)1097-4687(199701)231:1<63::AID-JMOR6>3.0.CO;2-P

Rose, C. (2009). Generating, growing and transforming skeletal shape: Insights from amphibian pharyngeal arch cartilages. *BioEssays*, *31*, 287–299. https://doi.org/10.1002/bies.200800059

Savage, R. M. (1950). Feeding mechanisms in anuran tadpoles. *Nature*, *166*, 155.

Schindelin, J., Arganda-Carreras, I., Frise, E., Kaynig, V., Longair, M., Pietzsch, T., Preibisch, S., Rueden, C., Saalfeld, S., Schmid, B., Tinevez, J. Y., White, D. J., Hartenstein, V., Eliceiri, K., Tomancak, P., & Cardona, A. (2012). Fiji: An open-source platform for biological-image analysis. *Nature Methods*, *9*(7), 676–682. https://doi.org/10.1038/nmeth.2019

Seale, D. B., & Wassersug, R. J. (1979). Suspension feeding dynamics of anuran larvae related to their functional morphology. *Oecologia*, *39*, 259–272.

Stöhr, P. (1882). Zur Entwickelungsgeschichte des Anurenschädels. *Zeitschrift für Wissenschaftliche Zoologie*, *36*, 68–103.

Tulenko, F. J., & Sheil, C. A. (2007). Formation of the chondrocranium of *Trachemys scripta* (Reptilia: Testudines: Emydidae) and a comparison with other described turtle taxa. *Journal of Morphology*, *268*(2), 127–151. https://doi.org/10.1002/jmor.10487

Warth, P., Hilton, E. J., Naumann, B., Olsson, L., & Konstantinidis, P. (2017). Development of the skull and pectoral girdle in Siberian sturgeon, *Acipenser baerii*, and Russian sturgeon, *Acipenser gueldenstaedtii* (Acipenseriformes: Acipenseridae). *Journal of Morphology*, *278*(3), 418–442. https://doi.org/10.1002/jmor.20653

Wassersug, R. J. (1975). The adaptive significance of the tadpole stagewith comments on the maintenance of complex life cycles in anurans. *American Zoologist*, *15*(2), 405–417.

Werneburg, I., & Yaryhin, O. (2019). Character definition and tempus optimum in comparative chondrocranial research. *Acta Zoologica*, *100*(4), 376–388. https://doi.org/10.1111/azo.12260

Ziermann, J. M., Mitgutsch, C., & Olsson, L. (2014). Analyzing developmental sequences with Parsimov—A case study of cranial muscle development in anuran larvae. *Journal of Experimental Zoology Part B: Molecular and Developmental Evolution*, *322*, 586–606. https://doi.org/10.1002/jez.b.22566

How to cite this article: Lukas, P. (2023). Embryonic pattern of cartilaginous head development in the European toad, *Bufo bufo*. *Journal of Experimental Zoology Part B: Molecular and Developmental Evolution*, *340*, 437–454. https://doi.org/10.1002/jez.b.23214